SF-98-12-3 (4108)

The Combined Effect of Air Leakage and Conductive Heat Transfer in Window Frames and Its Impact on the Canadian Energy Rating Procedure

Stéphane Hallé **Michel A. Bernier, Ph.D., P.E.**
Member ASHRAE

Armand Patenaude, P.E. **Robert Jutras, P.E.**

ABSTRACT

This paper examines the interaction between air infiltration/exfiltration and conductive heat transfer in window frames. This two-dimensional conjugate heat transfer problem is solved numerically using a finite-volume method. Two window frame geometries are examined with representative infiltration air leakage rates of 1.65 and 0.55 m^3/h per meter of crack length (0.3 and 0.1 ft^3/min per foot of crack). For each geometry, an aluminum frame with a PVC thermal break and a PVC frame are considered.

For the air infiltration case, the air-frame interaction causes the air to be preheated by the frame and decreases the apparent thermal transmittance of the frame. Conversely, air exfiltration increases the frame temperature, which increases heat losses, and the apparent thermal transmittance of the frame. When it is assumed that half the windows experience infiltration and the other half exfiltration, results indicate that the value of ER, calculated with a proper account of the air leakage-frame interaction, could be approximately 4.0 W/m^2(1.3 $Btu/h{\cdot}ft^2$) higher than the ER value calculated using the current CSA procedure (CSA 1993).

INTRODUCTION

Traditionally, the energy performance of windows was characterized by their thermal resistance. With recent advances in window technology, it has become apparent that thermal resistance alone is a poor indicator of the overall energy performance of a window. For example, air leakage through window frames and solar heat gains can have a significant impact on the annual amount of purchased energy required to compensate for window energy losses.

In Canada, an energy rating standard has been established for residential windows (CSA 1993). The calculation procedure given in the standard combines conduction losses, air leakage losses, and solar gains into a single value called the Energy Rating (*ER*) of the window. This value of *ER* gives the average heat gains/losses of a window over the entire heating season (5088 hours in Canada). The proposed Canadian energy code for houses (NRCC 1995) prescribes a minimum value of *ER* for each Canadian region. This value varies widely within Canada, ranging from +2 W/m^2 (0.63 $Btu/h{\cdot}ft^2$) in the Yukon to −24 W/m^2 (−7.61 $Btu/h{\cdot}ft^2$) in parts of British Columbia for operable windows.

Figure 1 presents schematically a house with two identical operable windows located on opposite sides. The enlarged version of the window on the left shows the three energy transfer modes used in the determination of the *ER* value: solar gains, conduction losses, and air leakage losses. Solar gains will not be examined here, but the treatment of conduction losses and air leakage losses in the current *ER* standard will now be briefly reviewed.

In the current rating procedure (CSA 1993), conductive heat losses are treated separately for three distinct areas of the window referred to as *center-of-glass*, *edge-of-glass*, and *frame*, as shown in Figure 1. The thermal transmittance associated with these three areas can then be combined to form an overall window thermal transmittance (ASHRAE 1993, chapter 27).

As shown in Figure 1, a gap is generally present in operable windows with one or more gaskets positioned in this gap to form a seal against air leakage. However, these gaskets are not perfect and windows will experience air leakage when they are subjected to a pressure differential. This pressure differential is dependent on wind and stack effects, and it varies along the height of the building (ASHRAE 1993). In the winter months, the maximum pressure differential caused by these two effects is around 4 Pa (CANMET 1996a). It should also be realized that when there is infiltration on one side of the house, there will be other parts of the house where air will exfiltrate.

Stéphane Hallé is a graduate student and **Michel Bernier** is associate professor at École Polytechnique de Montréal, Montréal, Québec, Canada. **Armand Patenaude** is president and **Robert Jutras** is general manager of Air-Ins Inc., Varennes, Québec, Canada.

BACK TO PAGE ONE

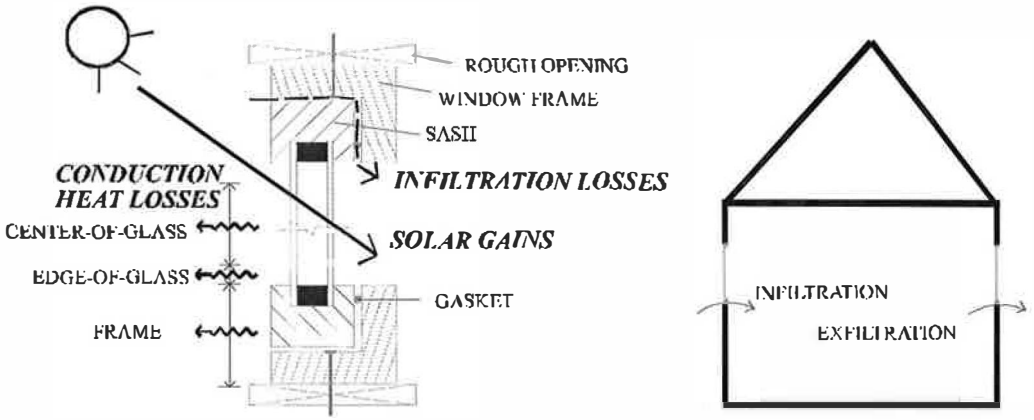

Figure 1 *Schematic representation of a window showing the various heat transfer modes.*

The current Canadian *ER* standard considers that air is unaltered as it flows through the window frame. Thus, air infiltration energy losses are given by the product of the mass flow rate times the air enthalpy difference between the inside and the outside. This product simply represents the amount of energy required to bring the outside air to room temperature. This implies that in the current Canadian *ER* standard, air exfiltration does not represent an energy loss since escaping air has already been heated. Based on these assumptions and assuming that window air infiltration and exfiltration are equal, the Canadian *ER* standard recommends the following equation (given here in SI units) to evaluate the *ER* value of a window for an averaged Canadian climate and for all cardinal points. The reader is referred to the CSA standard (CSA 1993) for a detailed discussion of this equation.

$$ER = 72.20F_w - \frac{(U_f A_f + U_{cg} A_{cg} + U_{eg} A_{eg})}{A_w} \times (t_i - t_o) - 0.0247 \frac{L_{75}}{A_w} \times (t_i - t_o) \quad (1)$$

where F_w is the solar heat gain coefficient; U_f, U_{cg}, and U_{eg} represent the thermal transmittance associated with the window frame, the center-of-glass, and the edge-of glass, respectively; A_f, A_{cg}, A_{eg}, and A_w represent the areas of the frame, the center-of-glass, the edge-of-glass, and the whole window, respectively; t_i is the indoor temperature; t_o is the averaged Canadian outdoor temperature during the heating season; and L_{75} is the window air leakage rate at a pressure differential of 75 Pa. The factor 0.0247 is a unit conversion factor that also accounts for the conversion of the window air leakage rate per meter of crack obtained at 75 Pa to a realistic window air leakage rate based on the work of Sherman and Grimsrud (ASHRAE 1993, chapter 23). In other words, the third term in Equation 1 represents averaged air infiltration/exfiltration energy losses. The resulting value of *ER* presented in Equation 1 is in W/m^2 and it represents the average heat gains/losses of a window over the entire heating season. The air leakage rate, L_{75}, is determined experimentally under isothermal conditions, 20°C (68°F) on each side of the window, at an air pressure difference across the window of 75 Pa, in accordance with ASTM Standard E283 (ASTM 1984).

The *ER* standard (CSA 1993) gives guidelines regarding the evaluation of each term in Equation 1. The evaluations of U_f and L_{75} will now be discussed briefly as they are the main focus of our investigation. First, for convenience, the terms that include F_w, U_{cg}, and U_{eg} are grouped into a constant, C, and the product $0.0247 \times L_{75}$ is replaced by $\dot{m}\, C_p$. Thus, Equation 1 takes the following form:

$$ER = C - U_f \frac{A_f}{A_w} \times (t_i - t_o) - \frac{\dot{m} C_p \times (t_i - t_o)}{A_w} \quad (2)$$

According to the *ER* standard (CSA 1993), the value of U_f can be calculated using a computer program called FRAME (CANMET 1996b). This program can calculate U_f for various geometries and boundary conditions, but it does not account for the interaction between air leakage and conductive heat transfer in the frame.

One of the major assumptions in the current *ER* standard is that the interaction between air leakage and conductive heat transfer in the window frame is negligible. Consequently, U_f and the product $\dot{m}\, C_p \times (t_i - t_o)$ are independent of each other. It is the objective of this paper to demonstrate that this assumption can be wrong under certain circumstances. To accomplish this task, the governing two-dimensional energy equation was solved numerically using a finite-volume method with a proper account of the resulting conjugate heat transfer between air infiltration/exfiltration and conductive heat transfer in the frame.

In the next section of this paper, modifications to the evaluation of the *ER* value are proposed to improve the accuracy of the current procedure. Then, the window frame geometries used in the present study are presented. This is followed by a presentation of the numerical methodology, including validation tests on the resulting computer code. Finally, comparisons are made between results obtained with the current *ER* standard and the proposed modifications for four different geometry/frame material combinations and two different air leakage rates.

BACK TO PAGE ONE

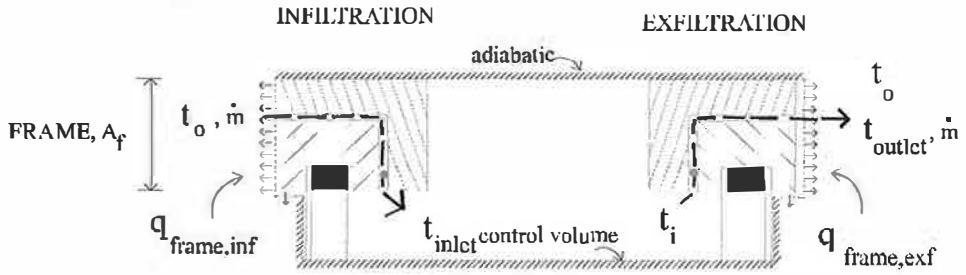

Figure 2 *Nomenclature used in the present study for the infiltration and exfiltration cases.*

PROPOSED MODIFICATIONS TO THE CURRENT EVALUATION OF *ER*

Under the proposed modifications, most of the current procedure would remain unchanged, except for the evaluation of U_f and the product $\dot{m}\,C_p \times (t_i - t_o)$, the last two terms in Equation 2. It is understood that U_{eg} would also probably be affected by the air leakage-frame interaction. However, for this study, conduction through the edge-of-glass was not considered.

In order to properly account for frame heat losses and air infiltration/exfiltration energy losses, a control volume has been drawn around two identical windows, as shown in Figure 2. The control volume consists of two adiabatic surfaces and two surfaces intersecting the outside surface of the two windows. Alternatively, the boundaries of the control volume could have been drawn on the inside surface of the two windows. The relevant energy flows are presented in Figure 2 and will now be briefly described.

Air enters the window frame on the left (infiltration case) at the outside temperature, t_o, with a mass flow rate $\dot{m}$. As it flows through the gap, the air is heated by the warmer frame and exists at a temperature t_{inlet}. The air is then heated by the house heating system to the room temperature, t_i. Frame heat losses for the infiltration case, $q_{frame,inf}$, are denoted by arrows crossing the control volume boundary located on the outside surface of the frame, as shown in Figure 2. For the exfiltration case, the air enters the frame with a mass flow rate and a temperature t_i. During its passage through the frame, the air is cooled by the relatively cooler frame and it leaves the frame at a temperature t_{outlet}. The frame heat losses for the exfiltration case, $q_{frame,exf}$, are also based on the outside surface, as shown by the arrows crossing the control volume in Figure 2.

The amount of energy required to compensate for frame heat losses and air infiltration/exfiltration energy losses in this two-window system, Q_{loss}, is given by:

$$Q_{loss} = -((U_{f,inf} + U_{f,exf}) \times A_f \times (t_i - t_o) + \dot{m} C_p \times (t_{outlet} - t_o)) \quad (3)$$

where $U_{f,inf}$ and $U_{f,exf}$ represent the effective thermal transmittance of the frame for infiltration and exfiltration cases, respectively. Considering that there are two windows in this analysis and that the value of *ER* is calculated per unit area, then the value of Q_{loss} should be divided by $2A_w$ when it is inserted in the *ER* equation. Thus, the proposed energy rating equation, denoted here by $\overline{ER}$, is given by

$$\overline{ER} = C - (U_{f,inf} + U_{f,exf}) \frac{A_f}{2A_w} \times (t_i - t_o) - \frac{\dot{m} C_p \times (t_{outlet} - t_o)}{2A_w} \quad (4)$$

The values of $U_{f,inf}$ and $U_{f,exf}$ are evaluated here by calculating the energy loss per unit area on the outside surface of the window frame, q_{frame}, divided by $(t_i - t_o)$. With reference to Figure 2, these effective thermal transmittance are given by

$$U_{f,inf} = q_{frame,inf} / (t_i - t_o)$$

and

$$U_{f,exf} = q_{frame,exf} / (t_i - t_o) \quad (5)$$

With these proposed modifications to the *ER* equation, $q_{frame,inf}$, $q_{frame,exf}$, and t_{outlet} need to be evaluated. In the present investigation, these values were obtained using a finite-volume computer code developed to account for conjugate heat transfer in window frames. The numerical methodology will be presented after the next section, which describes the window frame geometries used in the present study.

WINDOW FRAME GEOMETRIES

As shown in Figure 3, two window frame geometries were used in the present investigation. Two sets of materials were examined for each geometry: an aluminum-based frame with a PVC thermal break and a frame made entirely of PVC. In addition, L-shaped and Z-shaped gaps were examined.

The two geometries shown in Figure 3 may not represent the exact configuration of commercially available window frames. However, the objective of this investigation is to concentrate on the influence of air leakage on conductive heat transfer for simple realistic test cases. For this reason, influencing parameters, such as edge-of-glass heat transfer and temperature-dependent film coefficients, were not included in the analysis.

The values of t_i and t_o have been set at 20°C (68°F) and −1.9°C (28.6°F), respectively, in accordance with the *ER*

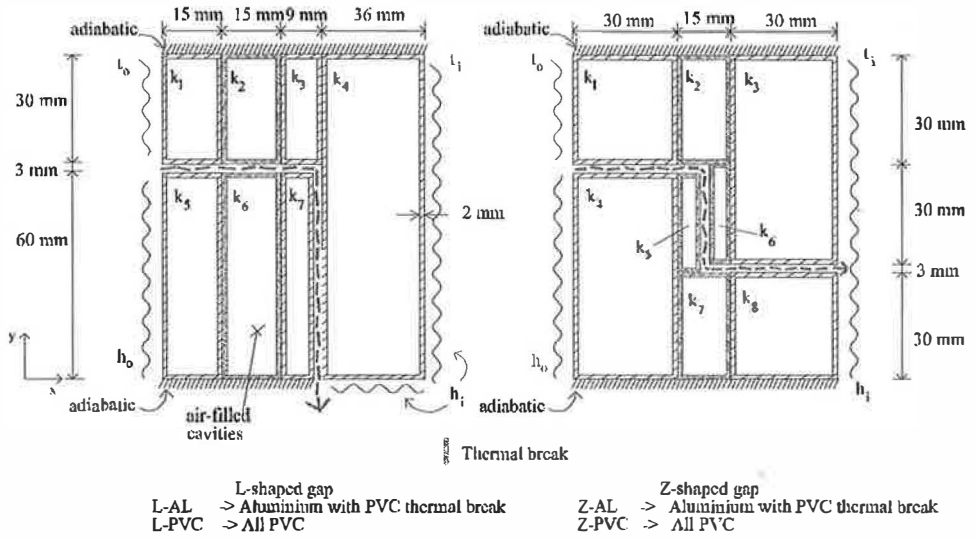

Figure 3 *Window frame geometries used in the present study. (To obtain dimension in inches divide the values given in mm by 25.4).*

standard (CSA 1993). The value of h_o was set at 30.0 W/m^2·°C (9.51 Btu/h·ft^2), while the value of h_i was fixed at 7.6 W/m^2·°C (2.41 Btu/h·ft^2) for the PVC frame and 7.9 W/m^2·°C (2.51 Btu/h·ft^2) for the thermally broken aluminum frame. Air properties in the gap were evaluated at a mean temperature of 11°C (51.8°F) giving values of 1.20 kg/m^3 (0.081 lb/ft^3) for density (Incropera and DeWitt 1990), 1.0 kJ/kg·°C (0.24 Btu/lb·°F) for specific heat, and 0.023 W/m·°C (0.0133 Btu/h·ft·°F) for thermal conductivity. The thermal conductivities of aluminum and PVC were set equal to 160 W/m·°C (92.5 Btu/h·ft·°F) and 0.17 W/m·°C (0.098 Btu/h·ft·°F), respectively. In order to limit the scope of this investigation and to concentrate on the air leakage-frame interaction, the complex radiative/convective heat transfers occurring in the air-filled cavities were not evaluated directly. Instead, the approach included in the current *ER* procedure was used. In this approach, effective thermal conductivities are obtained based on general correlations that account for the aspect ratio of the cavity and mean temperature (CANMET 1996b). The effective thermal conductivities k_1 to k_8 shown in Figure 3 and tabulated in Table 1 were obtained using this approach with the aforementioned boundary conditions.

TABLE 1
Effective Thermal Conductivities in the Air-Filled Cavities[a]

Thermal conductivities in W/m^2·°C	L-AL	L-PVC	Z-AL	Z-PVC
k_1	0.031	0.065	0.037	0.124
k_2	0.070	0.067	0.069	0.068
k_3	0.030	0.054	0.040	0.145
k_4	0.047	0.181	0.038	0.136
k_5	0.031	0.067	0.034	0.034
k_6	0.072	0.069	0.034	0.034
k_7	0.027	0.034	0.069	0.068
k_8	—	—	0.038	0.132

[a] To obtain the values of thermal conductivities in Btu/h·ft·°F, multiply by 0.578.

As shown in Figure 4, the overall dimensions of the window were set at 1220 by 600 mm (4 by 2 ft), which corresponds to a reference window size as determined by the *ER* standard. With these dimensions, the total crack length, l_c, is 3.4 m (11.15 ft), $A_f = 0.304$ m^2 (3.26 ft^2), and $A_w = 0.732$ m^2 (7.88 ft^2). Air leakage rates, L_{75}, of 1.65 and 0.55 m^3/h per meter of crack length (0.3 and 0.1 ft^3/min per foot of crack) were used for each geometry, which corresponds to mass flow rates of 1.39×10^{-4} and 4.62×10^{-5} kg/s, respectively. These leakage rates correspond to the upper limits of the A2 and A3

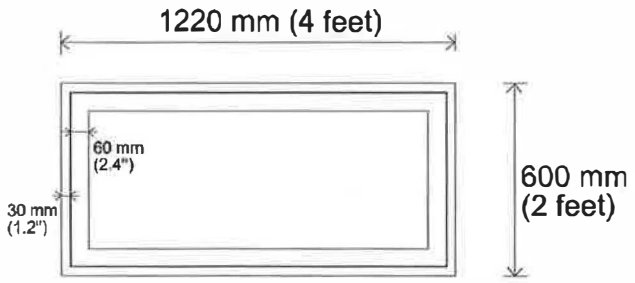

Figure 4 *Dimensions of the window under consideration as defined in the current ER procedure (CSA, 1993).*

classes of air leakage rates through windows (CSA 1990) under a 75 Pa pressure differential. Since most commercially available windows fit into one of these two categories, these air leakage rates can be considered to be representative of real situations. Finally, it is assumed that air leakage is distributed equally along the perimeter of both windows, which makes the problem two-dimensional. It could be argued that infiltration is greater in corners and that the resulting three-dimensional effects should be considered. However, to our knowledge, there are no available data in the scientific literature that describe infiltration asymmetry. Furthermore, considering that the current energy rating procedure (CSA 1993) neglects three-dimensional effects in corners in the determination of U_f, it was felt that the uniform leakage rate assumption was reasonable.

NUMERICAL METHOD

Governing Equation and Boundary Conditions

The numerical method used in the present study is based on the finite-volume method of Patankar (1980). Since this method is well known, only the salient features pertinent to this investigation will be presented. The present conjugate heat transfer problem involves the solution of the two-dimensional energy equation in the fluid and solid regions. This equation was obtained using the following assumptions: steady-state condition, constant properties in the fluid and solid regions, and fully developed laminar flow and negligible radiative heat transfer in the gap. Under these assumptions, the general governing equation is

$$\rho C_p u \frac{\partial T}{\partial x} + \rho C_p v \frac{\partial T}{\partial y} = k \frac{\partial^2 T}{\partial x^2} + k \frac{\partial^2 T}{\partial y^2} \qquad (6)$$

where T represents temperature, C_p is the specific heat, ρ is density, u and v are air velocities in the gap in the x and y directions, respectively, and k is the thermal conductivity. This general equation is used throughout the calculation domain with appropriate values of ρ, C_p, u, v, and k in the solid and fluid regions.

Three of the aforementioned assumptions need clarification. First, the assumption of laminar flow is fully justified considering that the Reynolds number, based on gap width, was never above 10. Secondly, even though the flow might be developing over a portion of the gap, the resulting velocity profile has no significant influence on conjugate heat transfer as shown in a related investigation of laminar mixed convection in tubes (LaPlante and Bernier 1996). Finally, the assumption of negligible radiative exchange between the walls of the gap is justifiable considering that both wall temperatures will be approximately equal at each axial location.

As shown in Figure 3, three types of boundary conditions are used: adiabatic, given temperature at the inlet of the gap, and boundary heat flux specified via a heat transfer coefficient, h_i or h_o, and the temperature of the surrounding fluid, t_i or t_o. The outflow boundary condition for the air exiting the gap is set as an adiabatic condition.

Equation Discretization and Solution Method

Integration of Equation 6 over a control volume around a point P in the calculation domain gives a discretized equation of the form:

$$a_p T_p = a_w T_W + a_e T_E + a_s T_S + a_n T_N + b \qquad (7)$$

where T_W, T_E, T_S, and T_N refer to temperatures at neighboring points. The coefficients a_p, a_w, a_e, a_s, and a_n were determined using a power law scheme (Patankar 1980). By applying this equation to each point of the calculation domain, a linear set of algebraic equations is obtained. This set was solved using a tridiagonal matrix algorithm (TDMA). The solution was considered to have converged when the sum of the absolute values of the relative changes in temperature at each node was below 10^{-8}.

Type-b grids (Patankar 1980) were used with control volume faces placed at the various fluid-solid and solid-solid interfaces, thus taking full advantage of the harmonic mean practice (Patankar 1980) for the interpolation of the thermal conductivities. The grid distribution utilized in this work was nonuniform in both directions. The grid points were concentrated where the largest temperature gradients were likely to occur. Based on the results obtained with grid independence checks, a typical grid size of 70 × 85 was used for both geometries with 7 and 3 grid points in the gap and in the wall of the cavities, respectively.

Validation

The equations and the solution methodology described above were implemented in a C++ computer code and executed using a 150 Mhz personal computer. Before using this code for the present study, a series of validation tests were

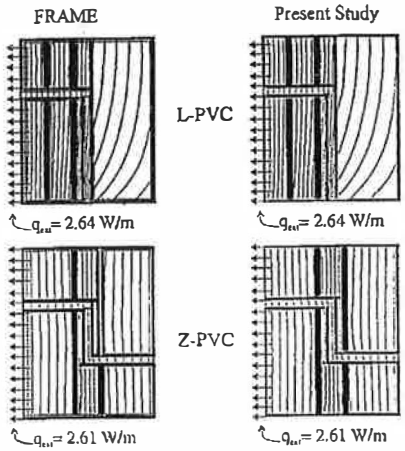

Figure 5 *Comparison of results obtained using FRAME and the code developed for the present study for a pure conduction case.*

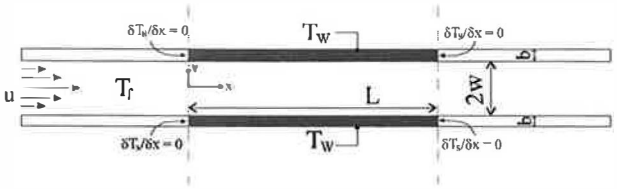

Figure 6 *Geometry used by Mori et al. (1976) in their study of laminar flow between two conducting parallel plates.*

performed. The results of two of these tests will now be presented.

The first validation check involved a comparison between the results obtained with the present code and the ones obtained using FRAME for a pure conduction case with the boundary conditions mentioned above. Figure 5 shows the resulting heat flux and isotherms obtained using both programs for both PVC geometries. The energy flows at the outside surface, given here in watts per unit depth, are identical for both programs. Due to different plotting utilities, the values of the isotherms presented in Figure 5 are not exactly the same for both programs; however, it can be seen that their shape is identical. Thus, the agreement between the results of these two programs is excellent.

In the second validation test, heat transfer to laminar flow between two conducting parallel plates was examined. This conjugate heat transfer problem was solved analytically by Mori et al. (1976). The geometry and the boundary conditions are presented schematically in Figure 6. As shown in this figure, the flow is bounded by a wall at $y = \pm w$, and the fluid temperature is equal to T_f for $x \leq 0$. In the central region, delimited by $0 \leq x \leq L$, a constant temperature condition ($T = T_W$) is applied at the outside surface of the wall. The thermal conductivity of the plate is k_s in the central region and is considered infinitely small elsewhere, resulting in an adiabatic boundary condition in the plate for $x = 0$ and $x = L$. Figure 7 presents the axial distribution of the dimensionless solid-fluid interface temperature in the central region as a function of K ($= k_s / k_f$), the ratio of solid to fluid thermal conductivities. As shown in Figure 7, both sets of results are in good agreement except near the entrance where a large number of grid points would have been required to handle the abrupt changes taking place at the entrance, especially for large values of K.

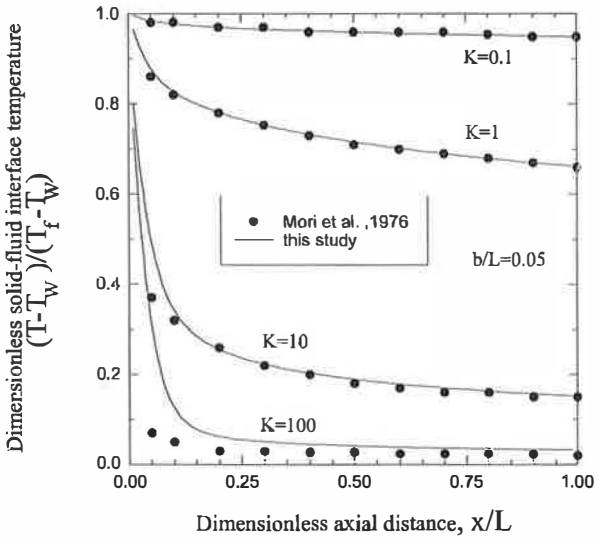

Figure 7 *Results of a comparison between the analysis of Mori et al. (1976) and the results of the present study.*

Based on these two validation tests, it was felt that the finite-volume method was correctly implemented and that the boundary conditions and the fluid-solid interface were handled properly. For the simulation results of the window frame test cases, which will now be presented, an overall energy balance was performed at the end of each simulation as a check for consistency. Typically, this balance was always verified within 0.5%.

RESULTS

Results obtained using the current *ER* standard and the ones obtained using the proposed modifications are summarized in Table 2. Values of U_f, $U_{f,inf}$, $U_{f,exf}$, t_{inlet}, and t_{outlet} are presented for 16 different simulations.

Since solar gains as well as edge-of-glass and center-of-glass conduction losses are considered identical for both the current procedure and the proposed modifications, they can be removed from the analysis by presenting results in terms of the difference in the value of *ER* given by both approaches. This difference, ΔER, ($= \overline{ER} - ER$) is presented in the last column of Table 2. Two intermediate values of ΔER are also presented in Table 2: ΔER_f represents the variation of ΔER attributable to the change in conductive heat losses in the frame, and ΔER_L corresponds to the variation of the energy lost by air infiltration/exfiltration. These values are given by:

$$\Delta ER_f = -\frac{(U_{f,int} + U_{f,ext})}{2A_w} A_f \times (t_i - t_o) + U_f \frac{A_f}{A_w} \times (t_i - t_o) \quad (8)$$

$$\Delta ER_L = -\frac{\dot{m} C_p \times (t_{outlet} - t_o)}{2A_w} + \frac{\dot{m} C_p \times (t_i - t_o)}{A_w} \quad (9)$$

with

$$\Delta ER = \Delta ER_f + \Delta ER_L \quad (10)$$

The first thing to note in Table 2 is that the value of ΔER is weakly dependent on the shape of the gap, with L-shaped and Z-shaped geometries giving essentially the same results. The value of ΔER is always positive, indicating that the current rating procedure (CSA1993) underestimates the value of *ER* and that less heating energy is required when the air leakage-frame interaction is taken into account. As shown in Table 2, this underestimation can be significant as ΔER reaches a value approximately equal to 4.0 W/m^2 (1.3 Btu/h·ft^2) for the A2 air .leakage rate. This difference can be traced back to the inter-

BACK TO PAGE ONE

TABLE 2

Summary of Results Obtained Using the Current *ER* Rating Procedure and the Proposed Modifications[a]

			Current Procedure		With proposed modifications						
Geometry	Air leakage rate	Leakage direction	U_f (W/m^2°C)	t_{inlet} or t_{outlet} (°C)	$U_{f,inf}$ or $U_{f,exf}$ (W/m^2 °C)	t_{inlet} or t_{outlet} (°C)	% difference in the value of U_f	(t_{outlet} - t_o) (K)	ΔER_f (W/m^2)	ΔER_L (W/m^2)	ΔER (W/m^2)
L-PVC	A3	INF.	1.29	−1.9	1.18	12.8	8.7%	1.5	0.0	1.4	1.4
		EXF.	1.29	20.0	1.39	−0.4	−8.2%				
L-PVC	A2	INF.	1.29	−1.9	1.06	12.5	17.6%	2.1	0.0	3.9	3.9
		EXF.	1.29	20.0	1.52	0.2	−18.4%				
L-AL	A3	INF.	2.91	−1.9	2.76	11.4	5.1%	2.3	0.1	1.3	1.4
		EXF.	2.91	20.0	3.03	0.4	−4.1%				
L-AL	A2	INF.	2.91	−1.9	2.68	11.2	7.9%	2.5	-0.1	3.9	3.8
		EXF.	2.91	20.0	3.15	0.6	−8.4%				
Z-PVC	A3	INF.	1.30	−1.9	1.21	15.7	7.1%	1.4	0.1	1.3	1.4
		EXF.	1.30	20.0	1.38	−0.6	−6.1%				
Z-PVC	A2	INF.	1.30	−1.9	1.10	15.1	14.9%	1.7	0.0	4.0	4.0
		EXF.	1.30	20.0	1.49	−0.2	−15.0%				
Z-AL	A3	INF.	2.90	−1.9	2.80	11.8	3.2%	2.2	0.2	1.3	1.5
		EXF.	2.90	20.0	2.95	0.3	−1.9%				
Z-AL	A2	INF.	2.90	−1.9	2.70	11.6	6.6%	2.3	0.1	3.9	4.0
		EXF.	2.90	20.0	3.08	0.4	−6.2%				

[a] To obtain BTU/h·ft·°F multiply the values given in W/m^2·°C by 0.1761; to obtain BTU/h·ft^2 multiply the values given in W/m^2 by 0.317.

action between air leakage and conductive heat transfer in the frame as will now be explained.

Infiltration Case

The infiltration case is illustrated in Figure 8 for the L-PVC-A2 combination. This figure presents isotherms resulting from numerical simulations (for clarity, solid boundaries have been omitted). As shown in Figure 8, the air is heated from t_o = −1.9 °C to t_{inlet} = 12.5°C showing clearly that the frame acts as a heat exchanger by preheating the infiltrating air. Furthermore, the outlet air reaches a temperature close to the average neighboring wall temperatures in the gap. For example, in the case of Figure 8, the wall temperatures on both sides of the gap at the outlet are approximately 10°C and 15°C for an average of 12.5°C. This closeness between air and averaged wall temperatures is due to the fact that the air leakage rates are relatively small so that the air is in the gap for a relatively long period, which gives it time to reach the averaged wall temperatures.

Since part of the energy that originates from convective heat transfer at the inside surface is picked up by the infiltrating air, there is less convective heat transfer at the outside surface ($q_{frame,inf}$) than when the air-frame interaction is not accounted for. Consequently, the apparent thermal transmittance of the frame, $U_{f,inf}$, is lower than U_f. As shown in Table 2, this decrease occurs in all cases and ranges from 3.2% to 17.6%.

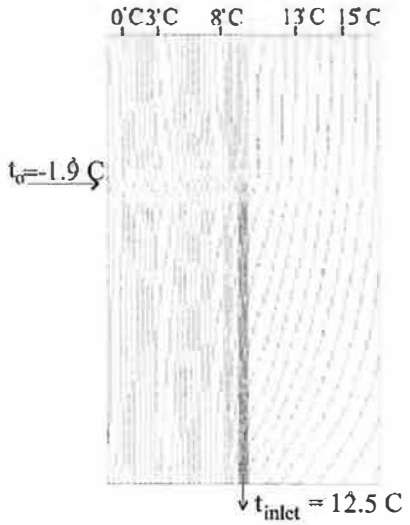

Figure 8 *Isotherms for the infiltration case of the L-PVC-A2combination.*

BACK TO PAGE ONE

Exfiltration Case

For the exfiltration case, the frame also acts as a heat exchanger. As shown in Table 2, the warm exfiltrating air (t_i = 20°C) is cooled by the relatively cooler frame, and t_{outlet} reaches values ranging from −0.6°C to 0.6°C. It can be shown, as was mentioned for the infiltration case, that the air at the outlet reaches the averaged wall temperatures at the gap outlet. However, in this case, t_{outlet} is closer to $t_o$than t_{inlet} was to t_i.This is because the outside film coefficient, h_o, is higher than the inside film coefficient, h_i. Consequently, the outside surface temperatures (including the surfaces near the gap exit) will be closer to t_o than the inside surface temperature is (including the surfaces near the gap exit) to t_i.

The values of $U_{f,exf}$ are higher than the values of U_f in all cases, with differences ranging from 1.9% to 18.4%, as shown in Table 2. This increase in the value of U_f can be explained by considering that the warm exfiltrating air increases the temperature on the outside surface of the frame, which increases $q_{frame,exf}$ and the resulting $U_{f,exf}$.

Impact on ΔER_L and ΔER_f

It is interesting to note that the increase in the value of U_f for the exfiltration case is approximately equal to the decrease in the value of U_f for the infiltration case, resulting in values of ΔER_f close to zero. This indicates that for the range of flow rates presented here the value of ΔER is mainly dependent on the value of ΔER_L.

The relatively small value of $(t_{outlet} - t_o)$ means that the air leaving the window for the exfiltration case is almost at the same temperature as the air entering the window for the infiltration case. Consequently, the first term in Equation 9 is relatively small compared to the second term, which is based on a higher temperature difference, $(t_i - t_o)$, of 21.9 K. Thus, the value of ΔER_L is mainly dependent on the second term of Equation 9.

Results presented in Table 2 also indicate that t_{outlet} is almost unaffected by an increase in air leakage rate with t_{outlet} remaining close to t_o in all cases. Consequently, the first term in Equation 9 remains small in comparison to the second term when the air leakage rate is increased from A3 to A2. Thus, it is not surprising to see the value of ΔER increasing by a factor close to 3 when the air leakage rate is tripled (from A3 to A2).

In summary, the results presented here show that the difference in the value of *ER* obtained with the proposed modifications and the current CSA standard, ΔER, is approximately equal to $\dot{m}\, C_p \times (t_i - t_o)/A_w$, which, it might be recalled, is equal to $0.0247\, L_{75} \times (t_i - t_o)/A_w$, the infiltration term in the definition of *ER* (Equation 1).

CONCLUSION

A new procedure has been proposed to evaluate the energy rating (*ER*) of windows that accounts for the combined effect of air leakage and conductive heat transfer. This conjugate heat transfer problem was solved numerically for two geometries, each with two air leakage rates and two frame material combinations.

When it is assumed that half the windows experience infiltration and the other half exfiltration, results indicate that the value of *ER* calculated using the proposed procedure could be approximately 4.0 W/m^2(1.3 Btu/h·ft^2) higher than the *ER* value calculated using the current CSA procedure (CSA 1993).

For the air infiltration case, the air-frame interaction causes the air to be preheated by the frame and decreases the apparent thermal transmittance of the frame. Conversely, air exfiltration increases the frame temperature, which increases heat losses and the apparent thermal transmittance of the frame. Furthermore, since the air leakage rates are relatively small, the air reaches the temperature of the neighboring wall surfaces as it leaves the gap for both the infiltrating and exfiltrating cases.

This paper has shown that the current Canadian energy rating procedure might underestimate the value of *ER* under certain circumstances. In our view, such findings should justify modifications to the current Canadian energy rating procedure to compare various window systems on a more realistic, fair, and accurate basis. Admittedly, a limited number of geometries were investigated and the presence of the insulated glazing unit was neglected. However, the results presented here indicate that the current values of *ER* should be used with caution until the full spectrum of window size-frame material-leakage rate combinations are examined.

ACKNOWLEDGMENTS

This research was financially supported by the Natural Sciences and Engineering Research Council of Canada and the Air-Ins company in the form of an Industrial Postgraduate Scholarship granted to S. Hallé and through an individual operating grant awarded to Prof. Bernier.

REFERENCES

ASHRAE. 1993. *1993 ASHRAE Handbook—Fundamentals*, SI edition. Atlanta: American Society of Heating, Refrigerating and Air-Conditioning Engineers, Inc.

ASTM. 1984. *Standard E283-84, Rate of air leakage through exterior windows, curtain walls, and doors.* American Society for Testing and Materials.

CSA. 1993. *Energy performance evaluation of windows and sliding glass doors*, CAN/CSA A440.2 and A440.3.Canadian Standard Association.

CSA. 1990. *Windows/user selection guide to CSA standard,* CAN/CSA A440-M90/A440.1-M1990.Canadian Standard Association.

CANMET. 1996a. Effect of window infiltration on annual energy use. Report prepared for NRCan/CANMET by Enermodal Engineering.

CANMET.1996b. Finite-difference computer program to evaluate thermal performance of window frame system, FRAME, Version 4.0. Enermodal Engineering Limited, Waterloo, Ontario, Canada.

BACK TO PAGE ONE

Incropera, F.P., and D.P. DeWitt. 1990. *Fundamentals of heat and mass transfer*, 3d ed. Wiley.

LaPlante, G., and M.A. Bernier. 1997. Convection mixte opposée et conjuguée dans un tube vertical. *Int. J. Heat Mass Transfer* 40(15):3527-3536.

Mori, S., T. Shinke, M. Sakakibara, and A. Tanimoto. 1976.Steady heat transfer to laminar flow between parallel plates with conduction in wall. *Heat Transfer*, Japanese Research, 5 (4): 17-25.

NRC. April 1995. National energy code for houses, second public review. Canadian Commission on Building and Fire Codes, National Research Council Canada.

Patankar, S.V. 1980. *Numerical heat transfer and fluid flow*. Washington, D.C.: Hemisphere.